

Why Fat Is Bright in RARE and Fast Spin-Echo Imaging¹

R. Mark Henkelman, PhD • Peter A. Hardy, PhD • Jonathan E. Bishop, BScE
Colin S. Poon, MSc • Donald B. Plewes, PhD

Fast spin-echo (FSE) sequences are becoming popular for T2-weighted clinical imaging because they result in a severalfold reduction in imaging time and because they provide conventional spin-echo contrast for most tissues. Fat, however, has been observed to have anomalously high signal intensity on FSE images. The present study shows that the brighter fat results from the multiple 180° refocusing pulses, which eliminate diffusion-mediated susceptibility dephasing and suppress J-coupling modulation of the echo train.

Index terms: Fat, MR • Phantoms • Pulse sequences • Rapid imaging

JMRI 1992; 2:533-540

Abbreviations: FSE = fast spin-echo, MEMP = multiecho multiplanar, RF = radio frequency.

HYBRID RARE (rapid acquisition with relaxation enhancement) (1), or, equivalently, fast spin-echo (FSE) (2), imaging has attracted considerable interest as the sequence of choice for T2-weighted clinical imaging. The advantages of FSE over conventional multiecho multiplanar (MEMP) imaging are an eight- or 16-fold decrease in imaging time through the use of different phase encoding for subsequent echoes in an eight- or 16-echo acquisition. Although the resulting T2-weighted contrast is variable over k space (3), it has been shown that the dominant image contrast is determined by the echo times of the low-order k-space acquisitions (4). By judicious choice of phase-encoding order and radio-frequency (RF) refocusing angle, contrast over k space can be made slowly varying, so that amplitude discontinuities and their associated ringing artifacts can be prevented. Contrast variations are further minimized by the accumulation of stimulated echoes in the later echoes of the multiecho acquisition (5-7).

Thus, hybrid RARE, or FSE, produces T2-weighted spin-echo images in considerably reduced time. The FSE images appear similar to MEMP images acquired with the same long TR/TE sequence that has become the clinical sequence of choice for identification of lesions. However, it has been noted that fat appears to have exceptionally high signal intensity on the FSE image relative to the equivalent MEMP image (8), as illustrated in Figure 1. Factors influencing this different contrast have been discussed by Constable et al (9).

It is the purpose of this report to show that the generation of multiple echoes in the FSE sequence is the cause of this increased signal intensity of fat and to consider possible mechanisms.

• MATERIALS AND METHODS

There are a number of specific differences between the MEMP and FSE sequences. To determine which of these differences is responsible for the increased signal intensity of fat on FSE images, we have developed several pulse sequences with properties that are intermediate between those of the MEMP and FSE

¹ From the Department of Medical Biophysics and Sunnybrook Health Science Centre, Research, University of Toronto, 2075 Bayview Ave. Toronto, Ont. Canada M4N 3M5 (R.M.H., J.E.B., C.S.P., D.B.P.); and the Cleveland Clinic Foundation, Cleveland (P.A.H.). Received April 28, 1992; revision requested May 28; revision received and accepted June 10. Supported by the National Cancer Institute of Canada, the Medical Research Council of Canada, and GE Medical Systems of Canada. J.E.B. is a recipient of an Ontario Graduate Scholarship. **Address reprint requests to R.M.H.**

© SMRI, 1992

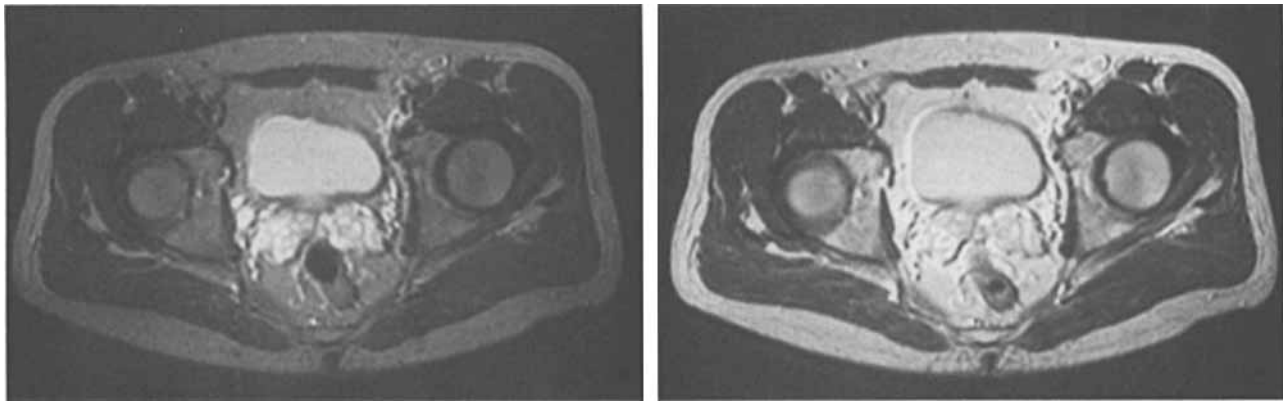


Figure 1. Same axial section through a normal pelvis imaged with conventional spin-echo (CSE) (a) and FSE (b) sequences. Imaging parameters: TR = 2,500 msec, TE = 80 msec, 192 × 256 matrix, 5-mm section thickness, two signals averaged. The CSE image (MEMP) was acquired in 16 minutes, whereas the FSE sequence used eight echoes and hence required only 2 minutes. The soft-tissue contrast seen on the CSE image is similar to that seen on the FSE image except that the fat is considerably brighter. Note that the seminal vesicles, which are bright on the CSE image, have the same signal intensity on the FSE image and have become isointense with fat.

Table 1
Experimental Imaging Pulse Sequences

Sequence	Varying Phase Encoding	No. of Echoes	Selective 180° Refocusing	Stimulated-Echo Spoilers	Phase Rewinding
MEMP	No	Single	Yes	Yes	No
Comp/single	No	Single	No	Yes	No
Comp/multi	No	Multiple	No	Yes	No
Sinc/multi	No	Multiple	Yes	Yes	No
Sinc/multi/rewind	No	Multiple	Yes	Yes	Yes
FSE	Yes	Multiple	Yes	No	Yes

Note.—Comp/single = composite pulse with single echo, comp/multi = composite pulse with multiple echoes, sinc/multi = sinc pulse with multiple echoes, sinc/multi/rewind = sinc pulse with multiple echoes and phase rewinding.

sequences. These pulse sequences are summarized in Table 1. The first two sequences are used in a single-echo mode only, and the final four are multiecho sequences with the number of echoes variable from two to 16. Four of the sequences use conventional selective 180° refocusing pulses, which consist of a single side-lobed sinc pulse of 3.2-msec duration modulated by a Hamming window. The other two sequences (comp/single and comp/multi) use a nonselective composite 180° refocusing pulse designed to be insensitive to B₀ and B₁ inhomogeneity (10). All sequences use the same initial 90° section-selective sinc excitation pulse.

The FSE sequence was the only sequence that did not include spoiler gradients along the section-select direction around the 180° pulses, since some of the performance of the FSE sequence depends on the development of stimulated echoes in the transition regions of the section-select profile to maintain signal intensity in later echoes. To distinguish the effects of section-selective spoiler gradients and phase rewinding, a sinc/multi/rewind sequence was used that incorporated both phase rewinding and gradient spoiling. This sequence can also be thought of as an FSE sequence with spoiling (11). Its behavior throughout was essentially identical to that of the sinc/multi se-

quence (without rewinding).

The first five sequences (Table 1) also incorporate section-selective spoiler gradients immediately before and after the 180° RF pulses. For the single-echo MEMP sequence, the spoilers consisted of a pair of gradient pulses of the same polarity as the section-select pulse, with the gradient pulse after the 180° excitation incorporating the compensation for the original 90° excitation. The second, third, fourth, and fifth pulse sequences used a more sophisticated spoiler pattern designed for T2 imaging (12), which was more effective in eliminating all stimulated echoes from larger (more than four echoes) multiecho sequences. This spoiler pattern is similar to that proposed by Crawley and Henkelman (13), except that the pattern of incremental spoiler gradients is reversed to a decremental spoiler pattern. The complete spoiler pattern would serve to contribute less than ±5° of diffusion-mediated dephasing. Although a standard multiecho MEMP sequence could have been used in place of the sinc/multi sequence (fourth sequence in Table 1), the sequence we have designed gives more flexibility with regard to the number of echoes and echo spacing and ensures superior stimulated-echo suppression.

All six sequences were used in a single-section

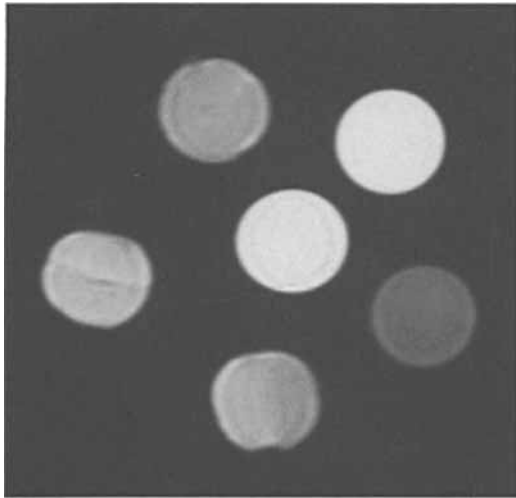


Figure 2. Coronal image of a phantom with tubes containing water doped with 0.3 mmol/L manganese chloride (center), vegetable oil (upper right), and, counterclockwise, pork fat (inner layer), pork fat (outer layer), a tube of mixed inner and outer pork fat, and, at the lower right, diethyl ether. All sample tubes were immersed in a beaker filled with water to minimize bulk-susceptibility effects.

mode on a Signa 1.5-T imager (GE Medical Systems, Milwaukee). A phantom consisting of six samples in 27-mm-diameter cylindrical tubes was imaged (Fig 2) with the following parameters: coronal section (zero offset), 128×256 matrix, two acquisitions with standard phase cycling of the 90° excitation, 24-cm field of view, 10-mm section thickness, transmit-receive head coil, and a TR for all experiments of 2,000 msec but with varying TE and number of echoes. Signal intensity was measured in a region of interest that encompassed 80% of the tube area.

The sample tubes contained water doped with 0.3-mmol/L manganese chloride, vegetable oil (Crisco), three samples of freshly excised pork fat, and diethyl ether (to demonstrate J-coupling). Where possible, the samples were designed to have a similar T1 and T2, as summarized in Table 2. The pork fat samples consisted of (a) a sample obtained immediately subcutaneously (outer fat), which was firm and lardlike; (b) a sample obtained from a fat layer between the outer fat and muscle (inner fat), which was blubbery; and a sample that contained equal amounts of the two types of fat, to demonstrate contrast between them.

To study the mechanisms of signal intensity enhancement in fat, the complete room temperature (23°C) experiments were repeated at temperatures of 2°C , 11°C , 16°C , 23°C , 31°C , 37°C , 43°C , and 52°C .

● RESULTS

Figure 3 shows signal intensity measured at room temperature as a function of TE for each of five phantom materials, with all six pulse sequences. For the multiecho sequences, the time between the 180° pulses was fixed at 20 msec. For the single-echo sequences, the TE was that recorded on the abscissa. From these results, several observations can be

Table 2
Relaxation Characteristics of Phantom Materials

Material	T1(msec)	T2(msec)
Doped water (0.3mmol/L manganese chloride)	440 ± 2	47 ± 1
Vegetable oil	209 ± 5	136 ± 4
Pork fat (inner layer)	208 ± 10	120 ± 3
Pork fat (outer layer)	207 ± 10	111 ± 3
Diethyl ether	$5,019 \pm 10$	N/A

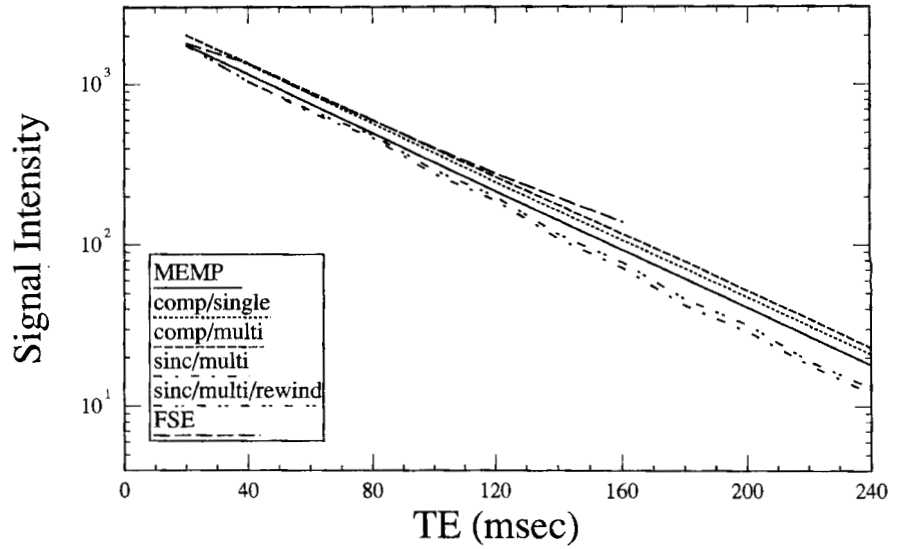
Note.—Oil and fat decay curves are multiexponential; the values quoted are linear averages. N/A = not available.

made. For doped water (Fig 3a), the signal intensities were similar with all pulse sequences except for those of the sinc/multi and sinc/multi/rewind sequences, which were considerably below the others at longer TE values. This decrease was due to the well-known progressive degradation of the section-excitational profile with application of repeated section-selective 180° pulses (12–14), resulting in a signal loss of about 9% per echo. Even the single-echo MEMP data were about 9% below the data from the comp/single sequence. The signal intensity at the initial point (TE = 20 msec) for the four sequences using sinc 180° pulses was 9% below that of the two sequences with composite pulses. This section-degradation effect of selective 180° pulses was seen throughout the study.

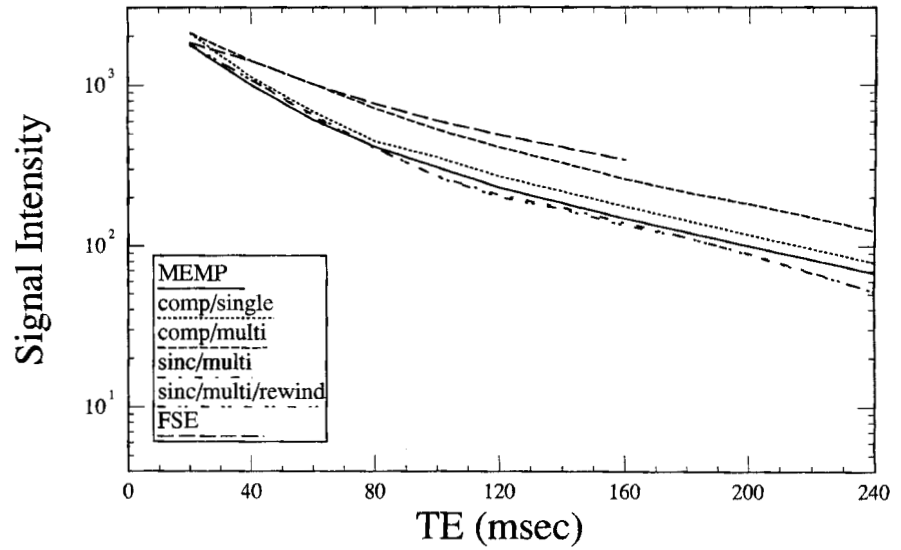
The vegetable oil (Fig 3b) showed a more interesting pattern of behavior. Relative to the MEMP data, signal intensities obtained with the comp/single sequence were again consistently higher by about 9% because of the greater efficiency of the composite 180° pulses. The major difference was between the comp/single and comp/multi sequences, with the multiple pulse sequence giving signal intensities 50% greater than those obtained with the single pulse sequence for TEs greater than 60 msec. Since identical (except for the number of RF excitations) nonselective refocusing pulses were used in the two sequences, both avoided section-profile effects. Therefore, it can be only the additional refocusing pulses that gave rise to the increased signal intensity. This is the main cause of bright fat on FSE images and will be the major consideration of the remainder of this report.

Compared with the comp/multi sequence, the sinc/multi and sinc/multi/rewind sequences showed decreasing signal intensity as the echo number increased, owing to section-profile degradation as discussed above. Finally, the signal intensity of the FSE sequence exceeded all the others. In fact, at a TE of 160 msec, the signal intensity of the FSE sequence was 2.6 times greater than that of the sinc/multi/rewind sequence. Therefore, allowing the stimulated-echo components to contribute to the signal rather than spoiling them makes a major contribution to the signal intensity. However, the FSE signal intensity exceeded even that of the comp/multi sequence, which preserves the initial section profile throughout. This additional enhancement is a J-coupling effect, which will be discussed below.

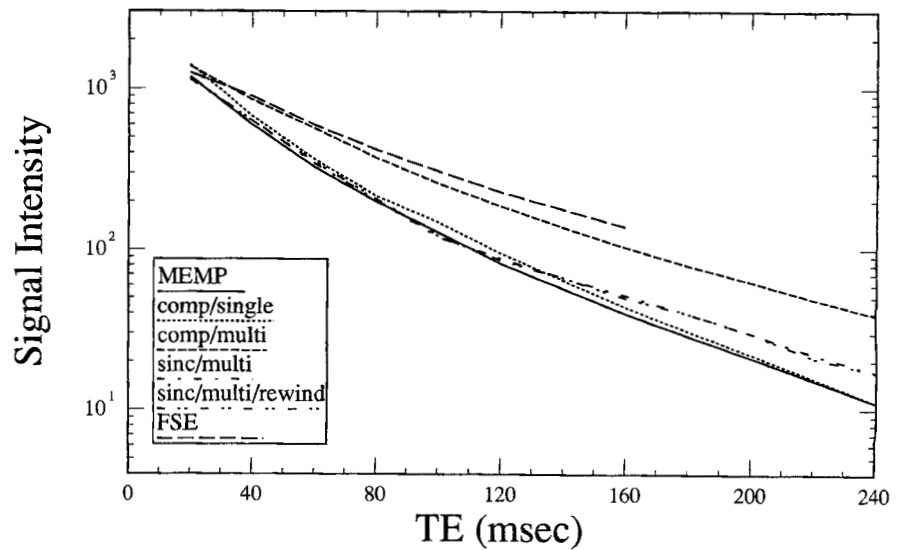
The pork fat samples (Fig 3c, 3d) showed similar behavior to that observed in the vegetable oil. The ma-



a.

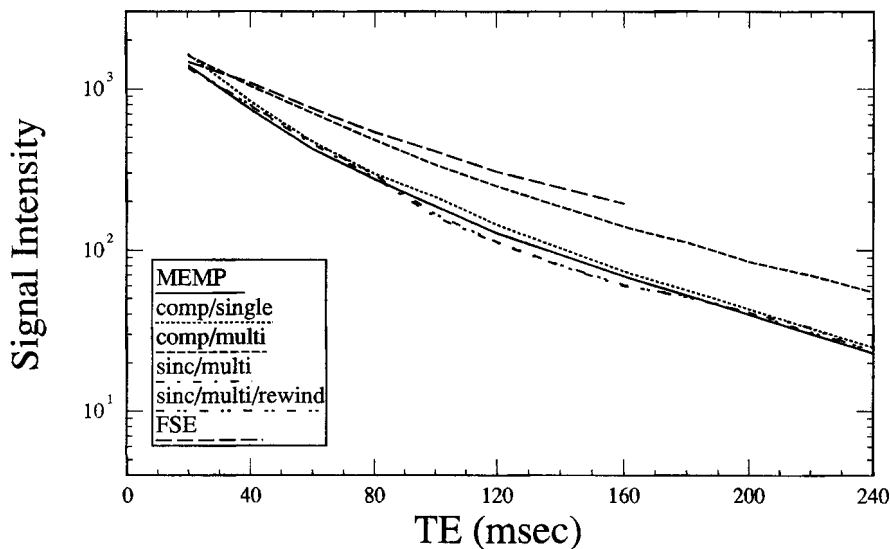


b.

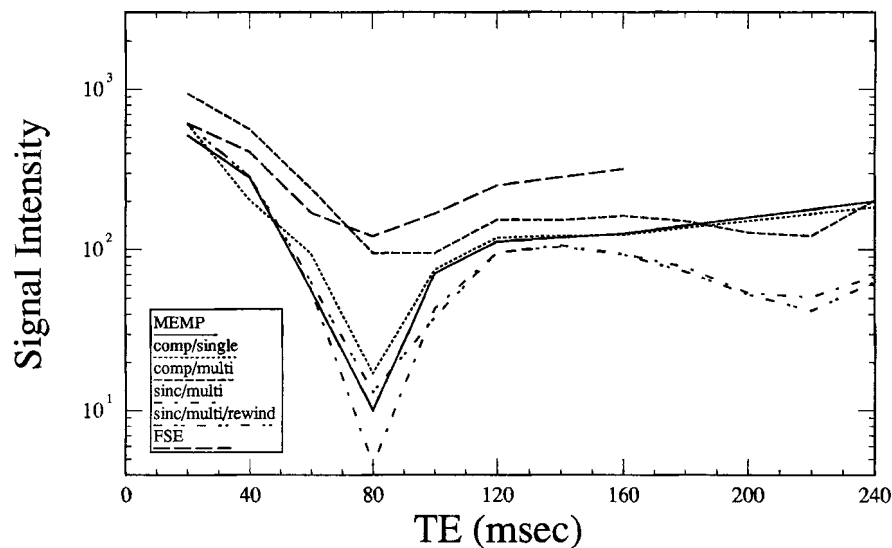


c.

Figure 3. Signal intensity versus TE for the six pulse sequences described in Table 1 for samples of (a) doped water, (b) vegetable oil, and (c) pork fat (inner layer) (Fig 3 continues).



d.



e.

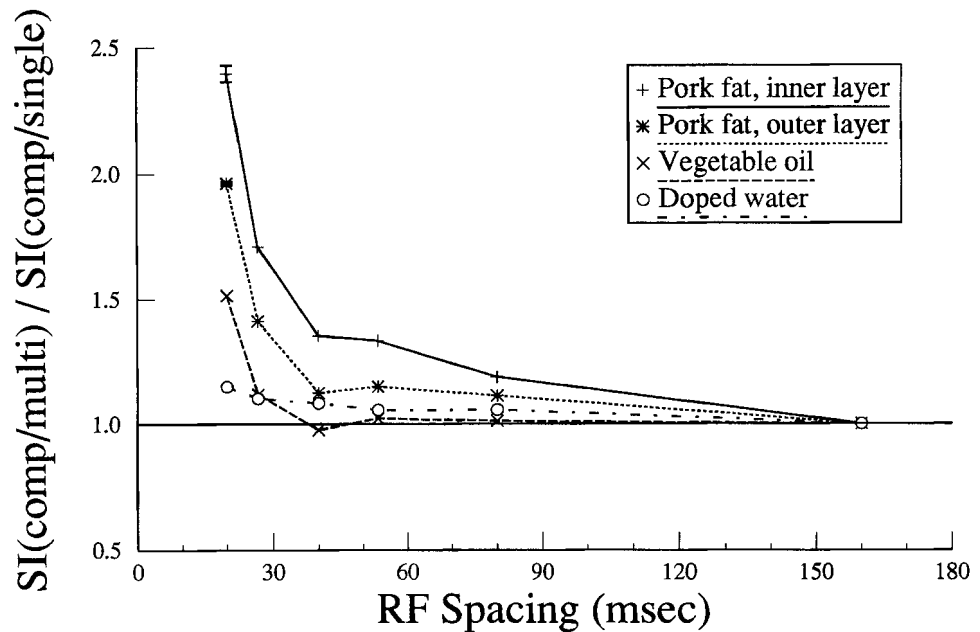
Figure 3 (continued). Signal intensity versus TE for the six pulse sequences described in Table 1 for samples of (d) pork fat (outer layer) and (e) diethyl ether.

For difference was that the comp/multi sequence signal intensity equaled or exceeded that of the comp/single sequence by factors that ranged from 1.0 for the first echo, at a TE of 20 msec (for this TE, the experiments were identical), to 1.6–1.7 at a TE of 80 msec and 1.9–2.4 at 160 msec and 2.2–3.5 times at 240 msec. This enhancement was substantially greater than that obtained in vegetable oil. Since pork fat is a macroscopically heterogeneous sample (unlike the oil), with susceptibility differences between the fat globules and water matrix, at long, single-echo TEs, diffusion-mediated dephasing of spins occurs as they move through local B_0 inhomogeneities (15,16). Multiecho sequences such as the sinc/multi sequence prevent this additional loss by restricting the effective time for diffusion. This additional mechanism did not occur in the oil sample because it was homogeneous; it was more evident in the inner layer of fat, which was visually more heterogeneous. The increase in signal

intensity of the FSE sequence relative to the comp/multi sequence was essentially equivalent to that seen in the vegetable oil.

Figure 3e shows the signal intensity patterns for diethyl ether, which showed marked J-coupling modulation. For this A_3B_2 system with a J-coupling of 7 Hz, one would expect the signal intensity to drop to zero at a TE of 72 msec, increase to about 20% of its full amplitude at a TE of 143 msec, return to zero at 215 msec, and then recover its T2-weighted value at a TE of 286 msec. This pattern can be seen qualitatively in Figure 3e for each of the single-echo sequences. It is well known that repeated 180° refocusing pulses will break the pattern of J-coupling modulation. This will occur when $\tau_{cp}\Delta \leq 1$, where $\tau_{cp} = TE/2$ and Δ is the chemical shift between the two spins. In the case of diethyl ether, $\Delta = 154$ Hz and thus J-coupling modulations will be substantially reduced for $TE \leq 12$ msec, as has been shown previously (17). Thus, for

Figure 4. Ratio of signal intensity for the comp/multi sequence to that of the comp/single sequence is plotted as a function of the 180° RF pulse spacing for four of the phantom materials: doped water, oil, and the inner and outer layers of pork fat. Error bars at the RF spacing of 20 msec are typical standard deviations over four repeat experiments (error bars for outer fat layer are smaller than symbol). All measurements were obtained at 23°C.



these experiments, in which the minimum TE is 20 msec, a decrease in the J-coupling modulation at shorter TEs is not particularly evident except in the comp/multi sequence and somewhat more in the FSE sequence. However, in fat and oil, in which the chemical shift between coupled spins can be much less, J-coupling modulation is considerably diminished at a TE of 20 msec.

Since the major feature seen in Figure 3 is the increased signal intensity in the comp/multi sequence relative to the equivalent comp/single sequence, and since this is the main effect contributing to bright fat with the FSE sequence, it is explored further in Figure 4. The ratio of the signal intensity of the comp/multi sequence to that of the comp/single sequence measured at a TE of 160 msec is plotted as a function of the 180° RF pulse spacing in the multiecho sequence. We have already discussed the results for an RF spacing of 20 msec, with water showing a ratio of 1.1, oil a ratio of 1.5, and pork fat a ratio of 1.9–2.4. The results for different RF pulse spacings are summarized in Figure 4. As the RF pulse spacing increases, the enhancement ratio decreases to approximately 1.0 for RF pulse spacings greater than 100 msec. At an RF pulse spacing of 160 msec, the two experiments are identical and the ratio of signal intensities is 1.0 by definition.

To help clarify the mechanism causing the results in Figure 4, the results of the temperature-dependence experiments are shown in Figure 5. For the doped water, the signal intensity ratio did not change with temperature. For the vegetable oil, the ratio dropped from 1.6 to 1.2 as temperature increased. However, for all oil and water samples, the apparent T2 and the signal intensity at a TE of 160 msec increased substantially at 50°C (approximately twofold) and decreased at 3°C (again approximately twofold) relative to room temperature, owing to decreases in

the effective correlation time with increased mobility at higher temperatures.

For fat, the enhancement of signal intensity with multiecho acquisitions was highly sensitive to temperature. The ratio of multiecho signal intensity at a TE of 160 msec with RF pulse spacing of 20 msec to the signal intensity of an equivalent single-echo acquisition was 2.0–2.4 at 23°C but decreased to 1.1–1.2 at 53°C. At temperatures lower than 23°C, the ratio continued to increase (outer fat) or even went through a maximum and decreased (inner fat). At 3°C, both types of fat become much more solidlike, with a substantial proportion (~50%) of their spins becoming invisible (Fig 5b) because of decreased mobility. The overall downward trend for the extrapolated proton density with temperature for water and oil (Fig 5b) is simply a reflection of the Boltzmann distribution, which determines the net equilibrium magnetization.

The large enhancement ratio of the multiecho to the single-echo measurement for fat at temperatures less than 30°C is therefore attributed to increasing susceptibility variation as the fat undergoes variable solidification. The multiecho sequence diminishes the susceptibility-induced dephasing in the spatially heterogeneous fat samples. The homogeneous water and oil samples do not show these anomalously high signal intensity ratios at lower temperatures.

● DISCUSSION

We have shown experimentally that the increased signal intensity of fat with T2-weighted sequences in FSE imaging relative to conventional spin-echo imaging arises from the train of 180° pulses that are used in FSE imaging. The signal enhancement does not occur in water but does occur in oil and, to a much greater extent, in fat. Furthermore, as seen on clinical images, it occurs to only a minor extent in muscle, brain, and any tissue that does not contain lipids, but

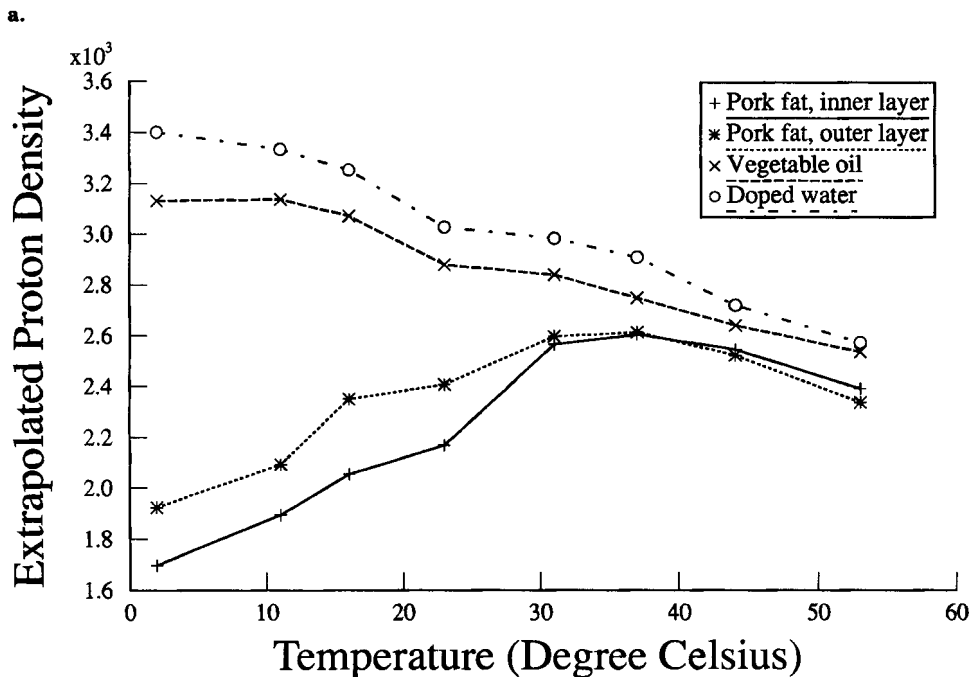
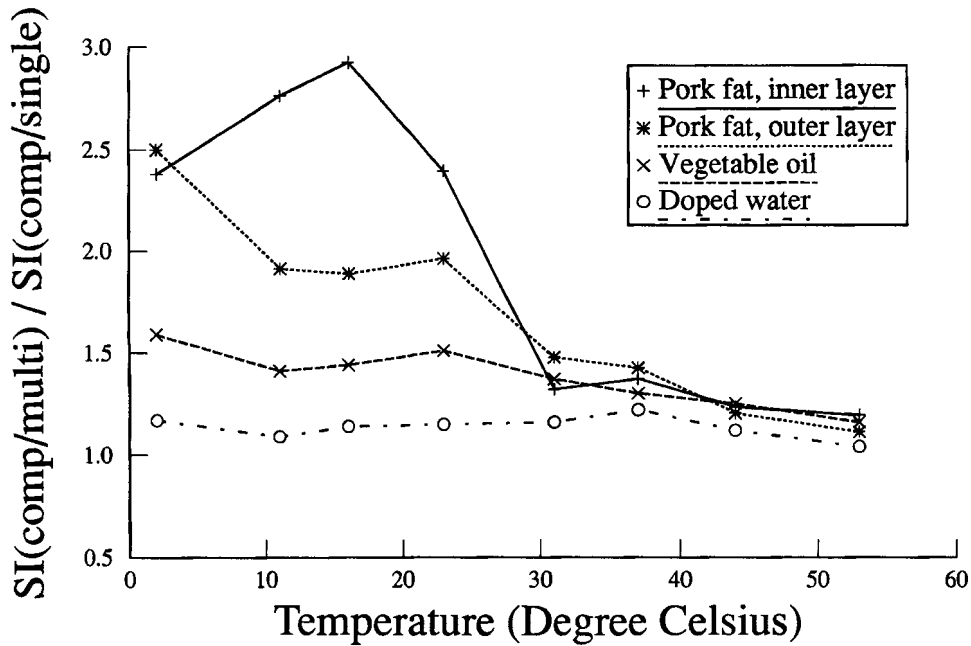


Figure 5. (a) Ratio of signal intensity of the comp/multi sequence to that of the comp/single sequence (at TE = 160 msec) is plotted as a function of temperature for water, oil, and the two pork fat samples. (b) The apparent proton density as determined from extrapolation to TE = 0 of the T2 decay curve for the comp/multi sequence is plotted as a function of temperature for the same four samples as in a.

it does occur in marrow and subcutaneous and peritoneal fat.

What then is the nature of the enhanced fat signal in FSE imaging? Three possible mechanisms are suggested: (a) chemical exchange or spin diffusion between sites with distinct chemical shifts, (b) elimination of J-coupling modulation of the echo train, and (c) proton diffusion through susceptibility-induced field inhomogeneities.

Chemical exchange of water protons and aliphatic protons, if it occurs, is likely to be modulated at RF

pulse spacings of less than 20 msec (18) and is, hence, unlikely to be responsible for the results seen in the present study.

A second possible mechanism arises from J-coupling. Homonuclear J-coupling in an AB system results in splitting of the chemically shifted lines into multiplets (19). As has been shown by Allerhand (20,21), Vold and Vold (22), Freeman and Hill (23), and Tokuhiko and Fraenkel (24), the Carr-Purcell decay is unmodulated even when there is strong J-coupling, provided that $|J| \tau_{cp} \ll 1$ and the chemical shift

is small relative to $1/\tau_{cp}$. This can be considered simply as a kind of "spin locking" (25). Thus, for sufficiently short τ_{cp} between the 180° refocusing pulses, the J-coupling modulation that is characteristic of single-echo acquisitions will be suppressed. A detailed quantitative theoretical analysis of the J-coupling effect and its disappearance as τ_{cp} approaches zero would be formidable for even a simple substance such as vegetable oil and has not been attempted by the authors for the much more difficult problem of fat.

The J-coupling mechanism is, however, independent of temperature (20–24). Therefore, the data in Figure 5 at 53°C lead us to conclude that the contribution to signal enhancement by J-coupling has an upper limit of 20%–30%. Enhancement greater than 30% must come from a mechanism other than J-coupling.

Because all the sequences are spin-echo sequences, static B_0 inhomogeneities will be rephased and not lead to signal modulation. However, diffusion in the presence of B_0 inhomogeneities produces diffusion-mediated signal loss with widely spaced refocusing pulses (16). This mechanism does not provide an explanation for the signal differences in oil, which is homogeneous in composition and thus possesses a homogeneous local field. However, in fat a substantial part of the enhancement with the FSE sequence must result from the multiecho elimination of signal loss due to diffusion through inhomogeneities. Certainly, at lower temperatures in fat, the inhomogeneities due to spatially varying solidification must be the major cause of signal enhancement with multiecho relative to single-echo sequences.

In conclusion, we have shown that the bright fat on FSE images relative to conventional spin-echo images is due to the multiecho refocusing train. We have shown that elimination of J-coupling modulation effects and, more important, desensitization of diffusion through inhomogeneities are contributing mechanisms to the unusual appearance of fat in FSE imaging. ●

Acknowledgments: This work is supported by the National Cancer Institute of Canada, the Medical Research Council of Canada, and GE Medical Systems of Canada. J.E.B. is a recipient of an Ontario Graduate Scholarship.

References

- Hennig J, Friedburg H. Clinical applications and methodological developments of the RARE technique. *Magn Reson Imaging* 1988; 6:391–395.
- Jolesz FA, Melki PS, Mulkern RV, et al. Clinical experience with fast spin echo imaging of the CNS (abstr). In: Book of abstracts: Society of Magnetic Resonance in Medicine 1991. Berkeley, Calif: Society of Magnetic Resonance in Medicine, 1991; 39.
- Twieg DB. The k -trajectory formulation of the NMR imaging process with applications in analysis and synthesis of imaging methods. *Med Phys* 1983; 10:610–621.
- Mulkern RV, Melki PS, Jakab P, Higuchi N, Jolesz FA. Phase-encode order and its effect on contrast and artifact in single-shot RARE sequences. *Med Phys* 1991; 18:1032–1037.
- Hennig J. Multiecho imaging sequences with low refocusing flip angles. *J Magn Reson* 1988; 78:397–407.
- Bishop JE, Plewes DB. Stimulated echo effects in fast echo images (abstr). In: Book of abstracts: Society of Magnetic Resonance in Medicine 1991. Berkeley, Calif: Society of Magnetic Resonance in Medicine, 1991; 1025.
- Hinks RS, Listerud J. Approach to steady state in fast spin echo imaging (abstr). In: Book of abstracts: Society of Magnetic Resonance in Medicine 1991. Berkeley, Calif: Society of Magnetic Resonance in Medicine, 1991; 1235.
- Melki PS, Mulkern RV, Panych LP, Jolesz FA. Comparing the FAISE method with conventional dual-echo sequences. *JMRI* 1991; 1:319–326.
- Constable RT, Anderson AW, Zhong J, Gore JC. Factors influencing contrast in fast spin echo MR imaging. *Magn Reson Imaging* 1992; 10:497–511.
- Poon CS, Henkelman RM. 180° refocusing pulses which are insensitive to static and radiofrequency field inhomogeneity. *J Magn Reson* (in press).
- Hennig J, Friedburg H, Stroebel B. Rapid nontomographic approach to MR myelography without contrast agents. *J Comput Assist Tomogr* 1986; 10:375–378.
- Poon CS, Henkelman RM. Practical T2 quantitation for clinical applications. *JMRI* 1992; 2:541–553.
- Crawley AP, Henkelman RM. Errors in T2 estimation using multislice multiple-echo imaging. *Magn Reson Med* 1987; 4:34–47.
- Majumdar S, Gore JC. Effects of selective pulses on the measurement of T2 and apparent diffusion in multi-echo MRI. *Magn Reson Med* 1987; 4:120–128.
- Stejskal EO, Tanner JE. Spin diffusion measurements: spin-echoes in the presence of a time-dependent field gradient. *J Chem Phys* 1965; 42:288–292.
- Hardy PA, Henkelman RM. On the transverse relaxation rate enhancement induced by diffusion of spins through inhomogeneous fields. *Magn Reson Med* 1991; 17:348–356.
- Hinks RS, Henkelman RM. Problems with organic materials for magnetic resonance imaging. *Med Phys* 1988; 15: 61–63.
- Grucker D, Mauss Y, Steibel J, Poulet P, Chambron J. Effect of interpulse delay on NMR transverse relaxation rate of tissues. *Magn Reson Imaging* 1986; 4:441–443.
- Abraham A. The principles of nuclear magnetism. Oxford, England: Oxford University Press, 1961; 499.
- Allerhand A. Analysis of Carr-Purcell spin-echo NMR experiments on multiple-spin systems. I. The effect of homonuclear coupling. *J Chem Phys* 1966; 44:2–9.
- Allerhand A. Modulation of Carr-Purcell spin-echo trains in homonuclear A_nBX_x systems. *J Chem Phys* 1969; 50: 5429–5430.
- Vold RR, Vold RL. Transverse relaxation in heteronuclear coupled spin systems: AX, AX₂, AX₃, and AXY. *J Chem Phys* 1976; 64:320–332.
- Freeman R, Hill HDW. Determination of spin-spin relaxation times in high-resolution NMR. In: Jackman LM, Cotton FA, eds. New York: Academic Press, 1975; 131–162.
- Tokuhiro T, Fraenkel G. Modulation of spin echoes in multi-half-spin systems. I. Closed formulas of Carr-Purcell spin echoes in several A_nBX_x systems. *J Chem Phys* 1968; 49:3998–4008.
- Santyr GE, Henkelman RM, Bronskill MJ. Variation in measured transverse relaxation in tissue resulting from spin locking with the CPMG sequence. *J Magn Reson* 1988; 79:28–44.